published in *Fundamental Aspects of High Temperature Corrsion VI*,
D. A. Shores, P. Y. Hou eds., (Electrochemical Society, Pennington, NJ, 1996) in press.

GRAIN BOUNDARY SEGREGATION OF CATION DOPANTS IN α-Al_2O_3 SCALES

B. A. Pint and K. B. Alexander

Oak Ridge National Laboratory,
P. O. Box 2008,
Oak Ridge, TN 37831-6156

Abstract

A Fe-20at%Cr-10%Al matrix was dispersed with a wide range of different oxides in order to study the effect of oxygen-active dopants on the high-temperature growth and adhesion of α-Al_2O_3 scales. The effect of these various cation dopants on the alumina scale microstructure has been correlated with dopant ion segregation to the α-Al_2O_3 grain boundaries using analytical electron microscopy. Elements such as Mn and V showed little effect on the oxide scale and were not observed to segregate. Elements such as Y and Gd resulted in finer, more columnar α-Al_2O_3 grains and were segregated to scale grain boundaries. However, Ti, Ta, Ca and Nb also were found to segregate but had a lesser effect on scale morphology. These results indicate that cation segregation to scale grain boundaries is not a sufficient condition to achieve beneficial oxidation effects. The driving force for segregation in growing alumina scales is discussed.

INTRODUCTION

Oxide-dispersed FeCrAl has been chosen as a model system (1-2) to study the reactive element (RE) effect on high-temperature oxidation (3-6). Using 0.2 cation% additions, 30 different dopants were added in order to assess parameters such as ion size and valence, and oxygen and sulfur affinities to determine why certain dopant elements produce beneficial effects on high temperature oxidation resistance.

It is now widely recognized that reactive element (RE) dopants in alloys segregate to the grain boundaries of externally-formed chromia (6-9) and alumina scales (6,10-16). The segregation is not as fine precipitates but as ions (6,15). With the use of cross-sectional transmission electron microscopy, the segregation of RE ions to the metal-scale interface also has been commonly observed (6,12-17). Despite the fact that segregation is a widely observed phenomenon, there is still debate as to the role these segregants play and little understanding of the driving force for the segregation.

A model (6) based on the role of RE ion segregation on oxidation behavior proposed that segregation at the metal-scale interface beneficially affected scale adhesion by suppressing the interfacial segregation of indigenous S, while segregation at the scale grain boundaries inhibited Cr or Al boundary diffusion and grain growth. The purpose of this study was to explore the latter relationship of grain boundary segregation and scale morphology in α-Al_2O_3 formed on model oxide-dispersed FeCrAl alloys. Microstructural observations were made on isothermally grown scales and segregation measurements were made on the same samples to correlate dopant effects.

Another unresolved issue is the driving force for segregation. Consequently, in this paper the scale segregation behavior is compared with segregation studies in bulk α-Al_2O_3 (18). Typically, lattice strain misfit of large ions in the close-packed α-Al_2O_3 lattice is cited as the driving force for segregation. It is also suggested that segregation may be driven by the oxygen potential gradient in the metal-scale-gas environment.

EXPERIMENTAL PROCEDURE

Gas-atomized Fe-20%Cr-10%Al powder and sub-micron oxide or nitride (vanadium) powders were mechanically blended in a flowing Ar atmosphere using a water-cooled, high-speed attritor and stainless steel balls. Standard dopant additions of 0.2 cation% were made. Lower additions were made in the case of Zr and La to avoid detrimental behavior associated with over-doping (1,19). Metal powder was milled without any dopant addition to create an Al_2O_3 dispersion. The blended powder was canned, degassed at 400°C, and extruded at 1100°C. For comparison, powders extruded without milling, cast Fe-20%Cr-10%Al, commercial ZrO_2-dispersed Fe-20%Cr-10.6%Al alloy (Kanthal alloy APM) and Y_2O_3-dispersed Fe-19%Cr-8.4%Al alloy (Inco alloy MA956) (13) also were included in the study. Chemical compositions are given in Table I.

Oxidation coupons (10-15 mm diameter x 1 mm thick) were polished to 0.3μm alumina and ultrasonically cleaned in acetone and methanol prior to oxidation. Isothermal oxidation experiments were conducted in dry, flowing O_2 at 1200°C with weight gains measured by a Cahn model 1000 microbalance. Exposures at 1300°C were conducted by placing specimens in pre-annealed alumina crucibles and oxidizing in air. Use of crucibles with lids allows for the collection and weighing of the spalled oxide from individual specimens. Specimen weight changes were measured before and after oxidation using a Mettler model AE240 balance. The focus of this work was the characterization of the oxide scale after oxidation using field emission gun, scanning electron microscopy (FEG-SEM) and energy dispersive x-ray analysis (SEM/EDXA). Selected specimens were analyzed using EDXA in a FEG transmission electron microscope (TEM) with a fine probe size (1-2nm). TEM parallel sections were prepared near the gas interface (20) to examine segregation at scale grain boundaries.

Table I. Chemical analysis of the as-extruded alloys. Dopant concentrations (in atomic percent) were determined by inductively-coupled plasma analysis. Sulfur and oxygen contents were determined by combustion analysis.

Addition:	dopant (at%)	S (ppm)	O (at%)	Other (at%)
Cast	<0.01 Y	52	0.009	<0.01 Zr
Extruded	0.006 Zr	25	0.08	0.003 Hf
Al_2O_3	<.001 Y	27	0.84	0.01 Ti
Ca	0.19	26	1.86	0.001 Zr
Ce	0.19	23	1.91	
Gd	0.19	24	1.86	0.01 Ti
Hf	0.19	27	1.89	
La	0.02	31	1.15	0.001 Y
Mg	0.19	20	1.40	
Mn	0.23	24	1.70	
Nb	0.19	22	1.99	
Nd	0.15	23	1.84	
Sc	0.16	29	1.79	
Si	0.48	27	1.80	0.001 Zr
Ta	0.17	21	1.93	0.02 Ce
Te	0.18	24	1.95	0.001 Y
Ti	0.20	22	4.46	
V(N)	0.20	28	1.10	0.002 Zr
Y	0.18	25	3.85	
Yb	0.17	25	1.81	
Y in MA956	0.30	110	0.66	0.39 Ti
Zr in APM	0.06	10	0.17	0.43Si

RESULTS

The α-Al_2O_3 scale formed on the various samples after 2h at 1200°C is a good example of the effect of the dopants on the scale morphology. Although the scale is rather thin (1-2μm), the structure is fully formed and the scale growth mechanisms on FeCrAl alloys are well-established (21-22). In general, with or without a RE addition, the scale is fairly flat under these conditions. At the scale-gas interface, the alumina morphology on undoped, Al_2O_3-dispersed FeCrAl (Figure 1a) is a fine ridge structure. These ridges presumably result from oxide growth at scale grain boundaries due to the outward boundary diffusion of Al (14). This same morphology is observed for the scale grown on undoped, cast FeCrAl and extruded FeCrAl alloys. It is also observed for several of the dopant cations including Mn, Si (Figure 1b), V, Te and Mg. The short whisker observed in Figure 1b is also consistent with the outward diffusion of Al.

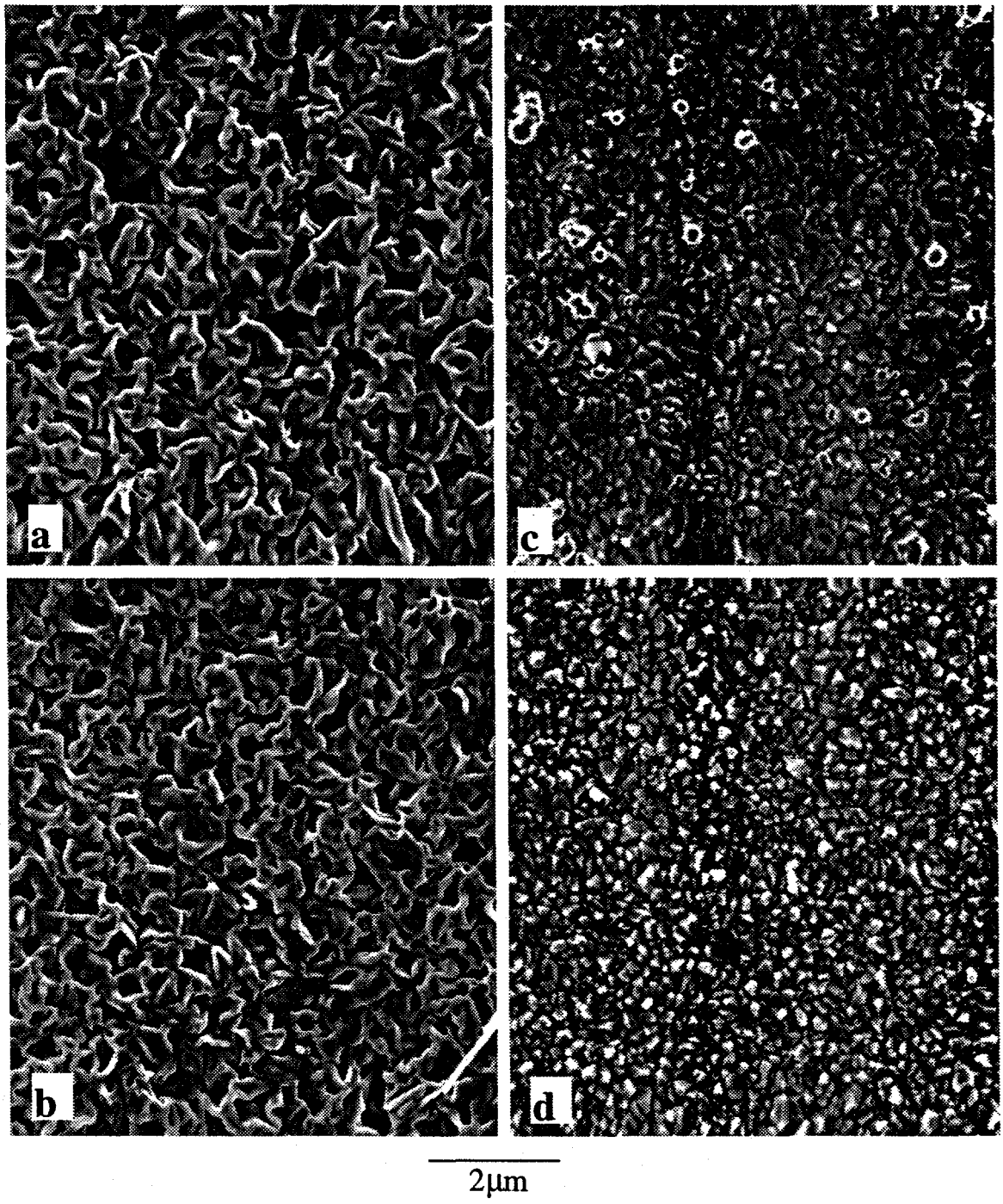

Figure 1. SEM secondary electron plan-view images of the alumina scale-gas interface formed after oxidation for 2h at 1200°C of Fe-20Cr-10Al with dispersions of (a) Al_2O_3, (b) SiO_2, (c) Y_2O_3, and (d) Gd_2O_3. With Y or Gd doping, the scale grain size is much finer and there is no ridge formation.

No ridges or whiskers are observed on the scale formed on Y_2O_3-dispersed FeCrAl (Figure 1c). Doping with Y results in a fine-grained surface structure. This same structure is observed for 0.2% additions of Nd, Ce, Gd (Figure 1d), Yb, Tb, Tm, Ho, Sm, Er, Lu and Dy. Additions of Sc, Eu and Hf also resulted in a fine-grain size but the scale was convoluted. This behavior has been associated with the addition of too much dopant, resulting in negative "over-doping" effects, such as an acceleration of the isothermal growth rate (1,2,19). Interestingly, reducing the amount of dopant eliminated the convolutions but also resulted in a coarser grain size or even a fine ridge network (23). The lower dopant levels may be insufficient to modify the scale microstructure or not uniformly dispersed, resulting in a partial effect. This was observed for the 0.06at%Zr addition in Kanthal alloy APM (14).

Not all of the dopants studied could be classified into the two general categories discussed above and shown in Figure 1. Additions of Ti, Nb, Ta and Ca resulted in intermediate behavior (Figure 2). Ti and Nb additions eliminated ridge formation but, unlike Y, did not produce a fine grain size. Ta and Ca additions produced a partial ridge structure, with less well-defined ridges than those observed in Figures 1a and 1b. The blade-like grains in Figure 2d were determined by SEM/EDXA to be rich in calcium. No metastable alumina phases were detected using glancing-angle x-ray diffraction. A summary of these observations of the scale surface morphology after 2h at 1200°C is given in Table II.

The other assessment of scale morphology effects was made on the through-thickness scale grain structure. Effective dopants not only produce a finer surface grain size after 2h at 1200°C but also produce a more columnar grain structure (24). The change to a columnar grain structure has been associated with the inhibition of Al boundary diffusion (6,21,22), resulting in growth primarily by the inward boundary transport of O. The effect on the through-scale grain structure is better illustrated on a thicker scale such as that formed after 100h at 1300°C. In fracture cross-sections, the scale formed on Al_2O_3-dispersed FeCrAl exhibits a fairly equaixed-grain structure and large internal voids are clearly visible (Figure 3a). This structure is typical of the dopants which showed little effect at 1200°C, such as Mn, V, Mg and Si. In contrast, the scale formed on Y_2O_3-dispersed FeCrAl, shows a very columnar grain structure with a much smaller grain size than the undoped scale (Figure 3b). This structure was also observed with additions of Ce, Nd (Figure 3c), Dy, Gd and Zr. As at 1200°C, there was a subset of dopants which resulted in convoluted scales (Table II). The partially effective dopants at 1200°C (Figure 2) did not produce a columnar grain structure. Additions of Ti, Nb, Ca and Ta (Figure 3d) appeared to have little effect on the grain structure at 1300°C.

Samples oxidized for 2h at 1200°C (the same samples as shown in Figures 1 and 2) were thinned to make TEM parallel sections near the gas interface of the scale. This was mainly a screening test to determine whether the cation additions segregated to the oxide grain boundaries. The qualitative results of these examinations are given in Table II. As might be expected, no segregation was observed for those scales which formed a ridged

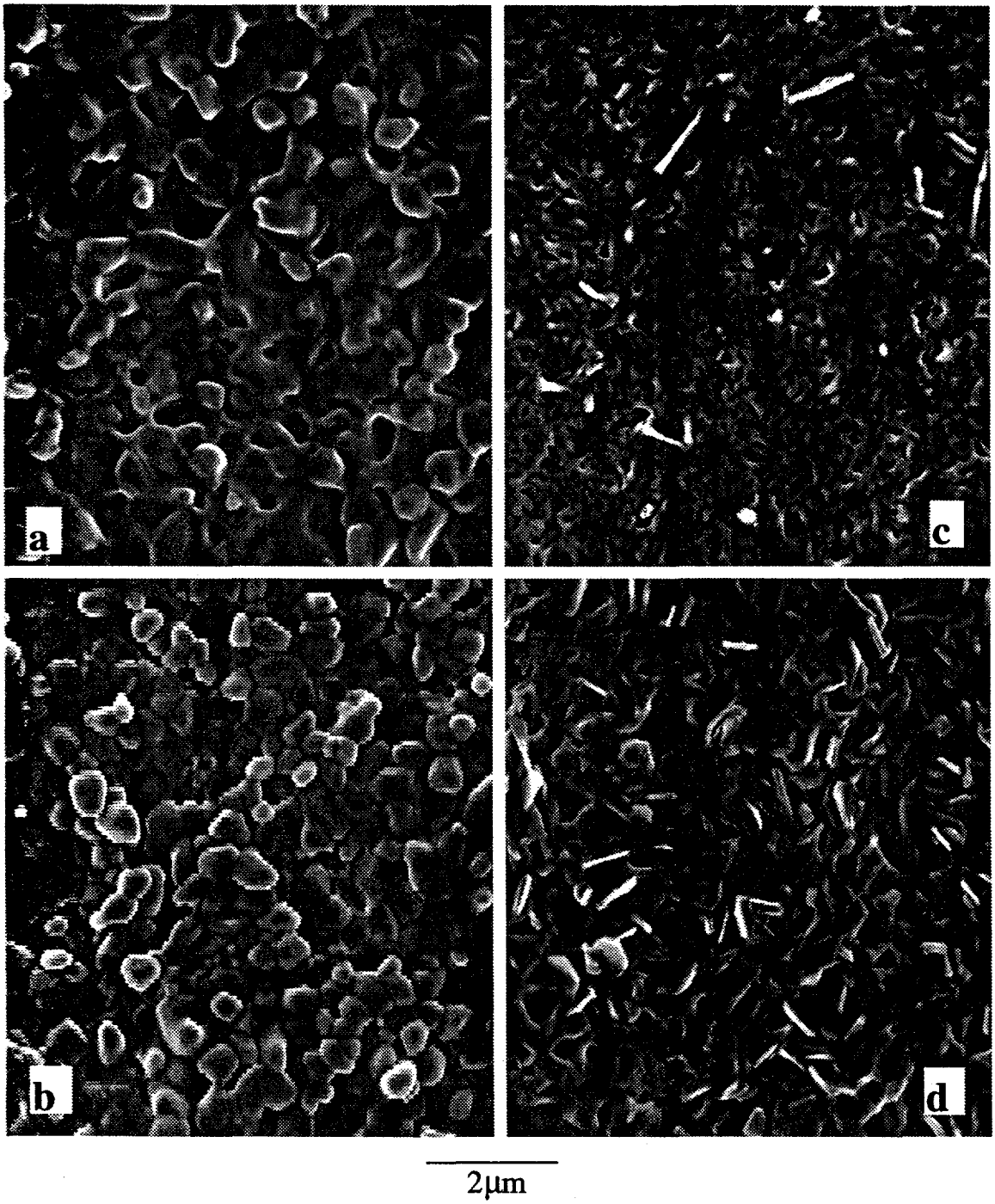

Figure 2. SEM secondary electron plan-view images of the alumina scale-gas interface formed after oxidation for 2h at 1200°C of (a) TiO_2-dispersed Fe-20Cr-10Al, (b) Nb_2O_5-dispersed Fe-20Cr-10Al, (c) Ta_2O_5-dispersed Fe-20Cr-10Al and (d) CaO-dispersed Fe-20Cr-10Al.

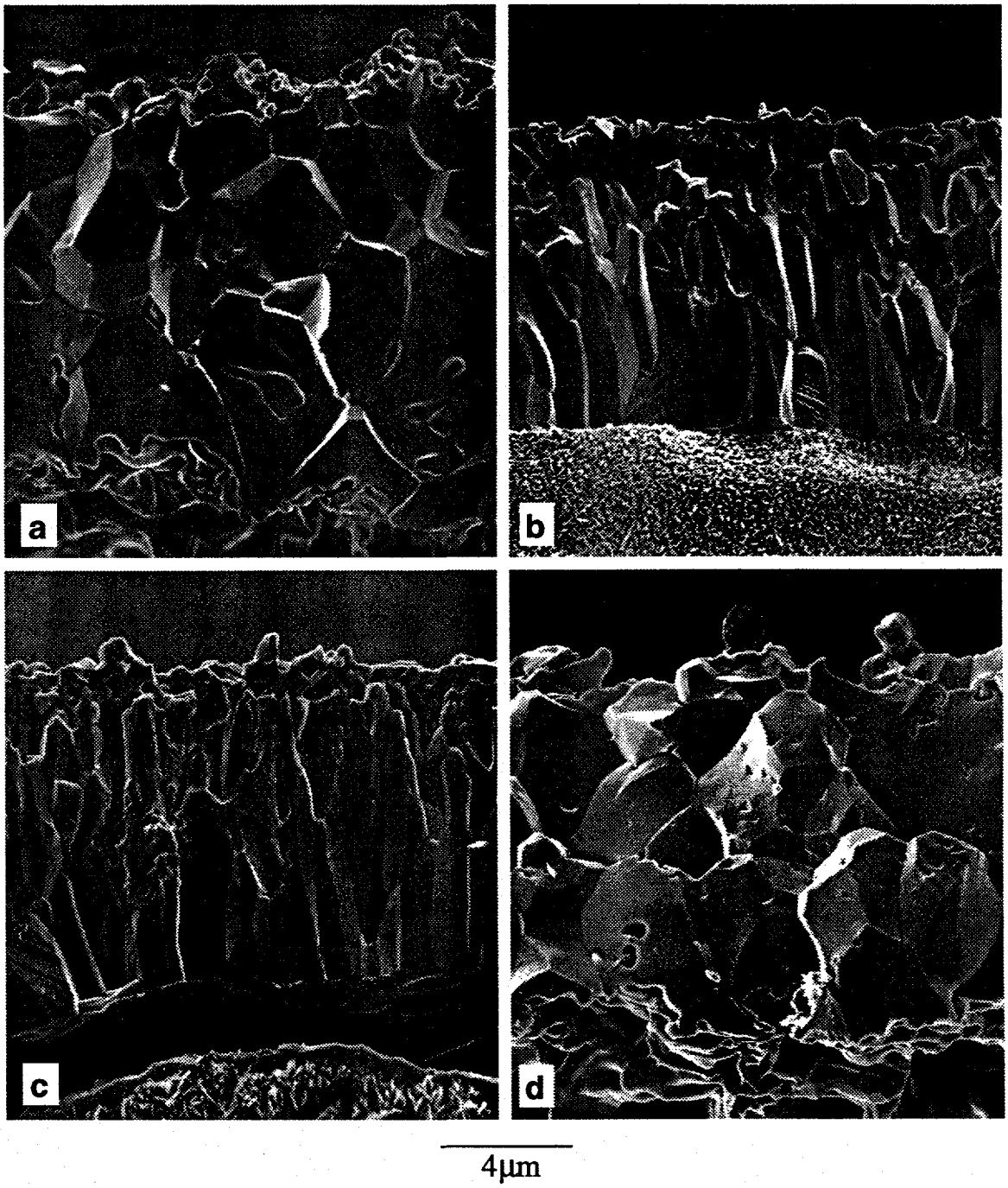

Figure 3. SEM secondary electron images of the α-Al_2O_3 scale formed after 100h at 1300°C on FeCrAl with a dispersion of (a) Al_2O_3, (b) Y_2O_3, (c) Nd_2O_3 and (d) Ta_2O_5. Additions of Y or Nd produce smaller grains with a more columnar structure.

structure similar to that observed on undoped FeCrAl (Figure 1). This includes Mg which is notoriously difficult to detect as a grain boundary segregant (18,25). In samples with fine-grained surface structures, segregation was detected in each of the scales examined. Of particular interest were the intermediate cases shown in Figure 2. In each of these specimens segregation was detected. Apparently, a foreign ion segregant is not a sufficient criterion for the formation of a fine-grained microstructure at the scale-gas interface. The thicker scales grown at 1300°C were not thinned for segregation studies. However, previous work at temperatures above 1200°C (13,16) has shown that those elements that segregate at 1200°C also segregate at higher temperatures. Thus it is expected that Ti, Ta, Nb and Ca also segregate at 1300°C but do not produce a columnar scale.

Table II. Current experimental results from the oxidation of oxide-dispersed FeCrAl with various cation additions.

FeCrAl with oxide dispersions of:	Nominal Cation Dopant Level (at%)	Detectable Grain Boundary Segregation after 2h at 1200°C	Gas-side Scale Morphology after 2h at 1200°C	Scale Grain Structure after 100h at 1300°C	Ionic Radius (Å) 6-fold coordi-nation
Undoped: cast extruded	N/A	N/A	ridges ridges	equiaxed equiaxed	N/A
Al	N/A	N/A	ridges	equiaxed	0.53
V(N)	0.2	Not detected	ridges	equiaxed	0.64
Si	0.2	n.t.	ridges	equiaxed	0.26[b]
Mn	0.2	Not detected	ridges	equiaxed	0.67[c]
Mg	0.2	Not detected	ridges	equiaxed	0.72
Ta	0.2	Yes	mixed	equiaxed	0.64
Nb	0.2	Yes	medium	equiaxed	0.72
Ti	0.2	Yes	medium	equiaxed	0.61
Ca	0.2	Yes	mixed	equiaxed	1.00
Sc	0.2	Yes	convoluted	convoluted	0.75
Hf	0.2	n.t.-Yes[a]	convoluted	convoluted	0.83[d]
La	0.025	n.t.-Yes[a]	mixed	convoluted	1.04
Yb	0.2	n.t.	fine	convoluted	0.87
Ce	0.2	n.t.-Yes[a]	fine	columnar	0.87
Nd	0.2	n.t.-Yes[a]	fine	columnar	0.98
Dy	0.2	n. t.	fine	columnar	0.91
Gd	0.2	Yes	fine	columnar	0.94
Zr in APM	0.06	Yes[e]	medium	columnar	0.84[d]
Y	0.2		fine	columnar	0.90
Y in MA956	0.3	Yes[e]	fine	columnar	0.90

n.t. : not tested
a : segregation observed in other alumina-formers, see Ref. 16
b : 4-fold coordination
c : for Mn^{2+}
d : 8-fold coordination
e : from Ref. 14

The driving force for foreign ion segregation is generally believed to be a reduction of strain misfit energy as large ions move from the lattice to the grain boundary. Aliovalent ions (particularly Ti) may also segregate due to a space charge effect (18). Thus it is not surprising that large dopant ions are also found to segregate at scale grain boundaries. However smaller ions should be less likely to segregate to these boundaries. For example, Sc_2O_3 and Al_2O_3 are reported to be miscible, yet Sc strongly segregates to the scale grain boundaries. To examine if this segregation was affected by the oxygen potential gradient of the growing scale, the TEM sample of the alumina scale grown on Sc_2O_3-dispersed FeCrAl was annealed for 100h at 1200°C in He-H_2 (to limit oxidation of the metal at the edge of the TEM sample). After annealing, the Sc segregation at the grain boundaries was unaffected, similar to that observed in Sc-doped bulk α-Al_2O_3 (18).

DISCUSSION

The present observations reveal several interesting points about the role of segregation in determining scale grain structure. The type of dopant has a large effect. Some dopants that segregate to the scale grain boundaries are not as effective in modifying the scale microstructure as others. This would appear to indicate that dopant segregation alone is not a microstructure-determining factor. However, the segregants which are not effective in altering the scale microstructure are somewhat different than typical RE additions such as Y, Zr and La. In particular, Ti, Nb and Ta are all smaller ions compared to the more effective dopants (Table II). Models involving grain boundary segregants are based on the ability of foreign ion segregants to effectively block the outward boundary transport of native cations and inhibit grain growth (6,7). These small ions may segregate but, due to their small size, are apparently unable to effectively inhibit cation diffusion and/or grain growth during oxidation. For example, Nb- and Ti- doping appear to inhibit scale ridge formation (Figure 2) but do not produce the same fine grain size as Y(Figure 1c). Thus, they may inhibit Al boundary transport (like Y) but do not inhibit grain growth to the same degree. Ta-doping is even less effective.

The addition of Ca also may be a special case. The rapid formation of Ca-rich precipitates at the gas interface (and their continued growth (2)) suggests that Ca diffuses rapidly through the scale (6,26). A fast diffusing foreign ion will be less able to block Al transport and inhibit grain growth. In fact Ca, unlike Mg, Y and La, is not a grain growth inhibitor in bulk alumina (25,27). Elements which significantly modify the scale microstructure tend to have a large ion size (relative to Ti, Nb and Ta, Table II) and a slow outward diffusion rate along the scale grain boundaries (relative to Ca) (6,16).

Comparison of segregation results in alumina scales to those for bulk alumina reveals some differences. Li and Kingery (18) analyzed 12 different dopants in bulk α-Al_2O_3 using FEG-STEM/EDXA. Unlike this work, they detected segregation of Mn and V to the grain boundaries. As an impurity, Si was also commonly detected as a segregant.

They concluded that the misfit strain energy of larger cations was the principal driving force for segregation. The results from bulk alumina indicate that all of the dopants studied in FeCrAl are segregants, thus annealing scales after oxidation would not likely change the segregation behavior of any element already present in the scale.

One difference between segregation behavior in bulk alumina and thermally-grown alumina scales is the role of the oxygen potential gradient on dopant diffusion in the latter (6,16). If the oxygen gradient helps to drive the diffusion of dopants from the metal to the gas interface (along the scale grain boundaries), then those with a high oxygen affinity would be more likely to diffuse from the metal into the scale and thus be more likely to be detected as segregants after oxidation. As a measure of oxygen affinity, the Gibb's free energies of formation for some relevant oxides are listed in Table III. Commonly, elements are ranked based on their free energy per mole of O, thus describing which are more likely to attract oxygen but this ordering does not correlate well with the segregation observations. However, in an oxygen potential gradient, the relevant factor is which cations are most attracted to oxygen. Thus, a second ranking is included of free energy per mole of cation. This ordering with the least stable oxide at the top and the most stable oxide at the bottom shows a better correlation: those elements with a higher cation affinity for oxygen than Al are those which are found to segregate to alumina scale grain boundaries. The low oxygen affinity of Mn and V relative to Al may explain why these

Table III. Gibb's free energy of formation for various oxides at 1500 K. When the cations are ranked in decreasing free energy (increasing oxide stability) per mole of cation, a different ranking is achieved then when ranked per mole of oxygen.

Cations: Ranking by affinity for oxygen	Oxide ΔG_f° (kJ/mole) per mole of Oxygen at 1500 K		Cations: Ranking by cation affinity	Oxide ΔG_f° (kJ/mole) per mole of Cation at 1500 K
Fe (Fe_2O_3)	-146.7		Fe	-220.1
V (V_2O_5)	-195.7		Mn	-275.5
Cr (Cr_2O_3)	-250.0		Cr	-375.1
Nb (Nb_2O_5)	-251.9		Mg	-425.5
Mn (MnO)	-275.5		Ca	-475.8
Ta (Ta_2O_5)	-281.0		V	-489.3
Si (SiO_2)	-307.2		**Al**	**-598.5**
Ti (TiO_2)	-338.8		Si	-614.5
Al (Al_2O_3)	**-399.0**		Nb	-629.8
Zr (ZrO_2)	-408.2		Ti	-677.7
Mg (MgO)	-425.5		Ta	-702.5
Ca (CaO)	-475.8		Zr	-816.5
Ce (CeO_2)	-518.7		Ce	-1037.4

elements were not detected as segregants in alumina scales but are found in bulk alumina. If there is no driving force for these elements to diffuse from the metal into the scale then they will not be present in the scale to segregate. The bulk alumina results suggest that if Mn and V were in the scale then they would be segregated at the grain boundaries. One exception to the ranking method is Ca, indicating this is not an absolute criterion. The driving force for segregation in scales remains an important issue as it relates to identifying the mechanism by which RE dopants improve oxidation behavior. More work will be required in order to link segregation behavior to the overall oxidation performance.

CONCLUSIONS

1. The type of dopant affects the grain structure of the α-Al_2O_3 scale formed on oxide-dispersed FeCrAl alloys.
2. The most effective dopants, such as Y, Nd and Gd, result in a finer, columnar grain structure and are found to segregate to the scale grain boundaries.
3. The least effective dopants, such as Mn, V and Si, do not change the scale morphology and are not found to segregate to the scale grain boundaries.
4. Certain elements, e.g. Ti, Nb, Ta and Ca, are found to segregate to the scale grain boundaries but have a lesser effect on the scale morphology.

ACKNOWLEDGMENTS

Research sponsored by the U.S. Department of Energy, Division of Materials Sciences, under contract DE-AC05-96OR22464 with Lockheed Martin Energy Research Corporation. BAP is supported by the Department of Energy Distinguished Postdoctoral Research Program administered by the Oak Ridge Institute for Science and Education.

REFERENCES

1. B. A. Pint, *Mat. Sci. Forum*, in press (1996).
2. B. A. Pint, "A Quantification of Dopant Effects in ODS FeCrAl," manuscript in progress.
3. F. H. Stott, *Mat. Sci. Forum*, **43**, 3 (1996).
4. D. P. Moon, *Mat. Sci. Tech.* **5**, 754 (1989).
5. R. Prescott and M. J. Graham, *Oxid. Met.*, **38**, 233 (1992).
6. B. A. Pint, *Oxid. Met.*, **45**, 1 (1996).
7. K. Przybylski and G. J. Yurek, *Mat. Sci. Forum*, **43**, 1 (1989).

8. C. M. Cotell, G. J. Yurek, R. J. Hussey, D. F. Mitchell and M. J. Graham, *Oxid. Met.*, **34**, 173 & 201 (1990).
9. N. Patibandla, T. A. Ramanarayanan and F. Cosandey, *J. Electrochem. Soc.*, **138**, 2176 (1991).
10. T. A. Ramanarayanan, M. Raghavan and R. Petkovic-Luton, *J. Electrochem. Soc.*, **131**, 923-31 (1984).
11. K. Przybylski, A. J. Garratt-Reed, B. A. Pint, E. P. Katz and G. J. Yurek, *J. Electrochem. Soc.*, **134**, 3207 (1987).
12. K. Prüßner, J. Bruley, U. Salzberger, H. Zweygart, E. Schumann and M. Rühle, in *Microscopy of Oxidation 2*, S. B. Newcomb and M. J. Bennett eds., p.435, Institute of Metals, London, U.K., (1993).
13. B. A. Pint, A. J. Garratt-Reed and L. W. Hobbs, *J. Physique IV*, **3**, C9-247-55 (1993).
14. B. A. Pint, A. J. Garratt-Reed and L. W. Hobbs, *Mat. High Temp.*, **13**, 3 (1995).
15. E. Schumann, J. C. Yang, M. J. Graham and M. Rühle, *Mat. and Corr.*, **46**, 218 (1995).
16. B. A. Pint, A. J. Garratt-Reed and L. W. Hobbs, "Oxygen Potential Gradient Enhanced Diffusion of Foreign Ions on α-Al_2O_3 Grain Boundaries," submitted to *J. Amer. Cer. Soc.*
17. K. Y. Kim, S. H. Kim, K. W. Kwon and I. H. Kim, *Oxid. Met.*, **41**, 179 (1992).
18. C. W. Li and W. D. Kingery, in *Structure and Properties of MgO and Al_2O_3 Ceramics*, Advances in Ceramics, 10, W. D. Kingery Ed., p.368, Amer. Cer. Soc. Inc., Columbus, OH. (1984).
19. B. A. Pint, P. F. Tortorelli and I. G. Wright, *Mat. and Corr.*, in press.
20. L. W. Hobbs and T. E. Mitchell, in *High Temperature Corrosion*, NACE-6, R. A. Rapp ed., p.76, NACE, Houston, TX, (1983).
21. W. J. Quadakkers, H. Holzbrecher, K. G. Briefs and H. Beske, *Oxid. Met.*, **32**, 67 (1989).
22. B. A. Pint, J. R. Martin and L. W. Hobbs, *Oxid. Met.*, **39**, 167 (1993).
23. B. A. Pint and K. B. Alexander, in *Microscopy of Oxidation 3*, G. Tatlock and M. J. Bennett eds., in press, Institute of Metals, London, U.K., (1996).
24. B. A. Pint, "The Morphology of Al_2O_3 Scales: Indicators of Phase Composition, Growth Mechanisms, and Grain Boundary Segregation," This Proceedings.
25. J. E. Burke, *MRS Bull.*, **21** (6), 61 (1996).
26. D. R. Sigler, *Oxid. Met.*, **40**, 555 (1993).
27. J. Fang, A. M. Thompson, M. P. Harmer and H. M. Chan, "Effect of Y and La on the Sintering Behavior of Ultra-High Purity Al_2O_3," submitted to *J. Amer. Cer. Soc.*